Frontiers in Scientific Research and Technology

Online ISSN: 2682-2970
Print ISSN: 2682-2962
http://fsrt.journals.ekb.eg

FSRT J 9 (2024) 1 - 13 10.21608/FSRT.2024.273633.1120

Geochemical characteristics and thermal maturity modelling of Alam El Bueib/Kharita in the Tut Oil Field, Shushan Basin, North Western Desert, Egypt.

Hadeer A. Hassan*[,1], Sherif Kharbish[1], Saada A. Saada[1], Naira M. Lotfy[2]

[1] Department of Geology, Faculty of Science, Suez University, P.O.Box: 43221, Suez, Egypt.

[2] Exploration Department, Egyptian Petroleum Research Institute, Ahmed El Zommor St. Nasr City, Cairo, 11727, Egypt

ARTICLE INFO

Article history:
Received 5 March 2024
Received in revised form 18 March 2024
Accepted 24 March 2024
Available online 26 March 2024

Keywords
Palynofacies,
Kerogen macerals,
Alam El Bueib/Kharita fms,
Thermal maturity model.

ABSTRACT

The main goal of this study is determining the source rock characteristics and petroleum generative potentiality of the Lower Cretaceous formations in the Tut Oil Field. The present work has employed multiple analytical techniques, including TOC, rock-eval pyrolysis, organic petrography, and palynofacies analysis. The geochemical analyses suggested that the Kharita Formation is immature source rock (with R_o= 0.52) with poor hydrocarbon potentiality to generate gas (type III and IV kerogen). The AEB Formation is ranging from immature to mature source rocks (with R_o= 0.52-0.67) and has poor to very good generating capability for producing gas and mixed oil/gas (III and II/III). Conversely, the organic petrographical analysis indicates that all samples of AEB Formation are of type II, with a high abundance of liptinite. Along with, Three palynofacies associations have been identified by the palynofacies study in the AEB Formation: Palynofacies association-A is dominated by the phytoclasts group, ranging from 54 to 90%, with significant amounts of amorphous organic matter (AOM) (6-38%), Palynofacies association-B reveals a high abundance of phytoclasts (61-98%) compared to palynomorphs and AOM, and Palynofacies association-C displays a dominance of AOM with significant amounts of phytoclasts. Ultimately, basin modelling was utilised to incorporate the results of geochemical tests in order to improve our understanding of the hydrocarbon production process from AEB/Kharita fms. According to this model, AEB Fm reached the early mature stage with a transformation ratio of less than 10% TR and no indications of generation or expulsion, while Kharita Fm are still in the immature stage.

1. Introduction

The Tut Oil Field is considered to be the most productive petroleum location in Egypt. It is situated in Egypt's northwest region of the Western Desert between latitudes 30° 44' 40" and 30° 46' N and longitudes 26° 57' 20" and 26° 59' 20" E (Fig. 1). The geochemical features of the Lower Cretaceous source rock qualities in the Tut Oil Field have been the subject of numerous investigations. El Nady (2001) revealed that the Lower Cretaceous source rocks are mature, of mixed organic matter (II/III), and have fair to good capability to generate gas and oil. The Early Albian Kharita Fm is considered to be an immature source rock of terrestrial origin and has poor to fair potential to produce gas. Sharaf and El Nady (2003) recognized that the Alam El Bueib (AEB) Formation has poor to fair potential to generate oil at optimum maturity in the south Umbraka area.

Ramadan et al. (2012) recognized that the AEB source rock in Tut Oil Field varies from poor to very good source rock rich with kerogen of type III and characterized by immature to mature rocks. El Nady and Hakimi (2016) showed the numerical modeling of single well (Tut-1x) indicates that the source rocks of AEB and Masajid formations entered the early-mature stage of oil-generation during the late Cretaceous time and persisted to present-day. This indicates that the AEB and Masajid source rocks have not been generated hydrocarbons.

Although, there is more previous studies have been undertaken on the Lower Cretaceous formations, this study discusses in details the organic matter characteristics of Lower Cretaceous source rocks in Tut Oil Field by employing TOC, Rock-Eval pyrolysis, palynofacies analysis, and organic petrological study. Subsequently, the thermal modelling will demonstrate the evolution of petroleum generation and expulsion from the Lower Cretaceous source rocks in Tut Oil Field.

* Corresponding author at Nuclear Materials Authority

E-mail addresses: Hadeer.Ali@sci.suezuni.edu.eg (Hadeer A. Hassan)

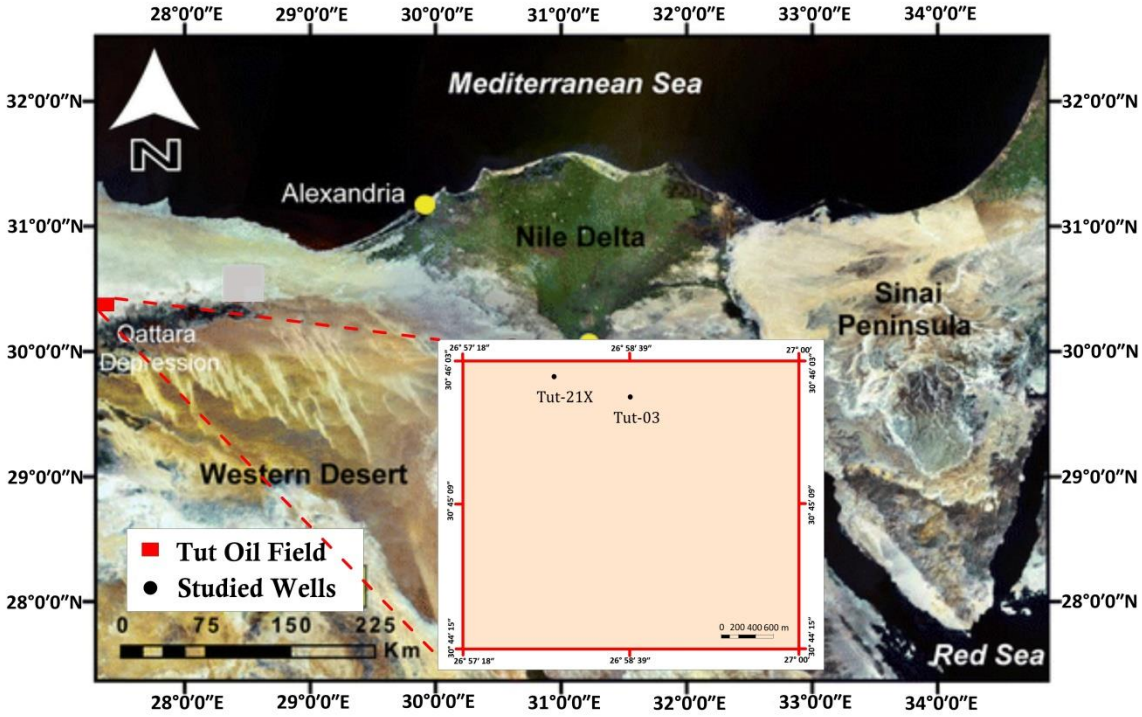

Fig. 1: A map showing the location of the studied wells in the Tut Oil Field, Shushan Basin, northern Western Desert, Egypt.

2. Geological setting

In the north section of the Western Desert, the Shushan Basin is located, which has a northeast-southwest trend. Comprising a considerable area of Egypt's unstable shelf, it spans around 3800 km^2 (Said, 1990). As illustrated in Fig. 2, the stratigraphic section of the northern Western Desert, which includes the Shushan Basin, represents ages ranging from Paleozoic to Tertiary. The Middle Jurassic, Lower Cretaceous, Upper Cretaceous, and Eocene to Miocene are the four unconformity-bound cycles that make up the strata. According to Sultan and Abdelhalim (1988), May (1991), EGPC (1992), Shalaby et al. (2013), and Yasser (2020), each of these cycles begins with fluvio-deltaic siliciclastics and finishes with marine carbonates. Only these intervals are of interest in this research: a) The AEB Formation, which is mostly made up of sandstone and shale and rests conformably on the Masajid Formation, contains small carbonate rocks that were deposited in a marine environment (Temraz et al., 2016). The six units that comprise its lithology are AEB-6, AEB-5, AEB-4, AEB-3, AEB-2, and AEB-1. The AEB-3 unit itself is divided into six components, which are G, F, E, D, C, and A. (b) The Kharita Formation consists of shallow marine sandstone and a few shale interbeds (Barakat, 1982). A large shallow marine shelf in a high-energy (mostly littoral) environment provided the origin of the Kharita Formation, which contains several carbonaceous shales with a high potential for gas production and a gas-prone nature (EGPC, 1992) (Fig. 2).

3. Materials and analytical techniques

These analyses took place out in the Stratochem Services Laboratory and the Egyptian Petroleum Research Institute laboratories. Forty-five (45) cuttings samples were received for geochemical analysis. All samples were solvent washed to eliminate the effect of mud additive contamination (Diesel), and then analysed for Total Organic Carbon (TOC) determination. Forty-four (44) samples with a TOC wt% greater than 0.5 were submitted for Rock Eval pyrolysis. Espitalié et al. (1977) provide a summary of interpretation criteria for Rock-Eval data, including details on the analytical process of the Rock-Eval parameters. After inspection of TOC and Pyrolysis data, three (3) samples were selected for kerogen microscopy analysis. In addition, four (4) samples were prepared for vitrinite reflectance examination (%VR_o) using a microscope with white light source, photometer and oil immersion objectives.

Thirty-four (34) samples from the AEB Formation in the Tut Field were prepared with the standard palynological method of Traverse (2007). Each sample is ground and sieved to remove silicates and carbonates by increasing the surface area of the reaction with HCl and HF. The residue was sieved to separate the unwanted rock from the finer kerogen residue. After that, a small amount of sample was evenly spread on a glass coverslip, and then the samples were left to dry, then mounted on a glass slide using Elvacite 2044 acrylic resin dissolved in xylene as a mounting medium. Transmitted light microscopy and Leica DMLS and Leica DFC 280 cameras were used to scan these slides for their kerogen content.

Finally, PetroMod (1D) petroleum system modelling software was used to simulate burial and thermal histories in order to build a maturation model of the Tut-21x well in the Tut Oil Field. Furthermore, the modelled vitrinite reflectance was calibrated using the measured vitrinite reflectance (R_o %). As well as the timing of hydrocarbon generation was decided based on the kinetics of the estimated kerogen type for each formation (Pepper and Corvi, 1995).

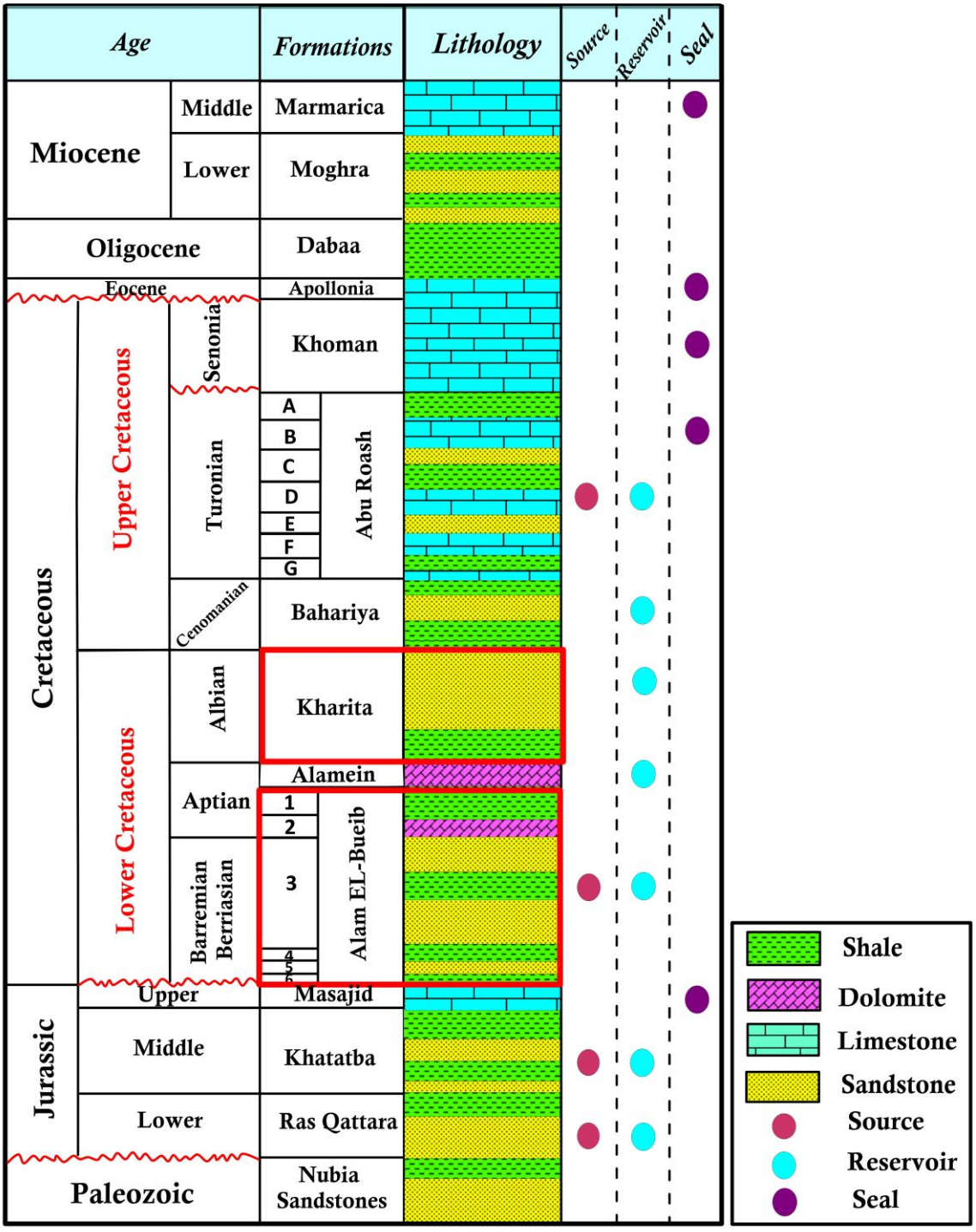

Fig. 2: Stratigraphic column of the northern Western Desert, including the Shoushan Basin (Shalaby et al., 2012). The study formations are represented by the red rectangle.

4. Result and Discussion

4.1. The generative potential of source rock

One important indicator of a source rock's ability to produce hydrocarbons is its organic matter abundance (Huang et al., 2010). Total organic carbon (TOC wt %) is a common way to express the organic richness of a rock. For clastic type rocks with good source potential, a minimum acceptable TOC value is 1.0% (Peters and Cassa 1994; Hunt, 1995). The Lower Cretaceous Kharita Formation has TOC wt% content in the range of 0.62–1.40. Meanwhile, the TOC of the AEB Formation ranges between 0.54 and 3.62.

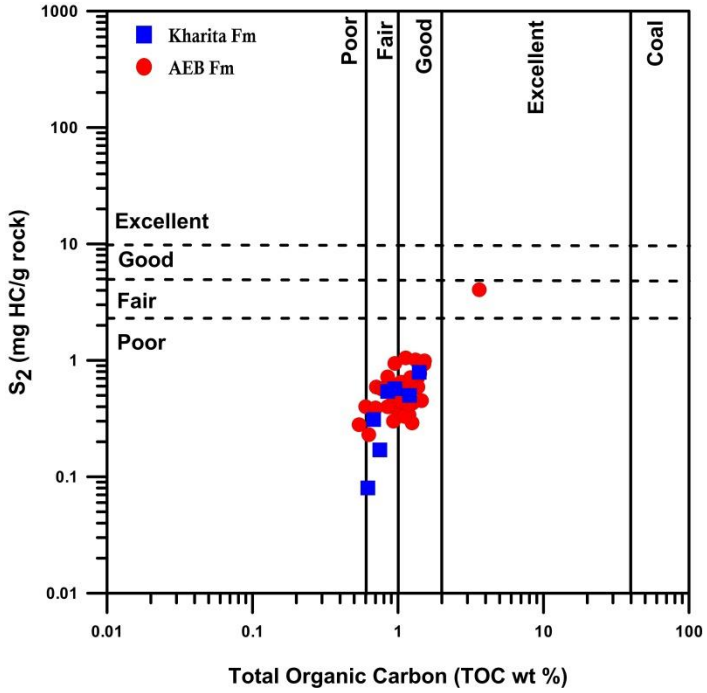

Fig. 3: The TOC% versus S_2 mg HC/g rock cross-plot shows the hydrocarbon generative potential of the studied samples.

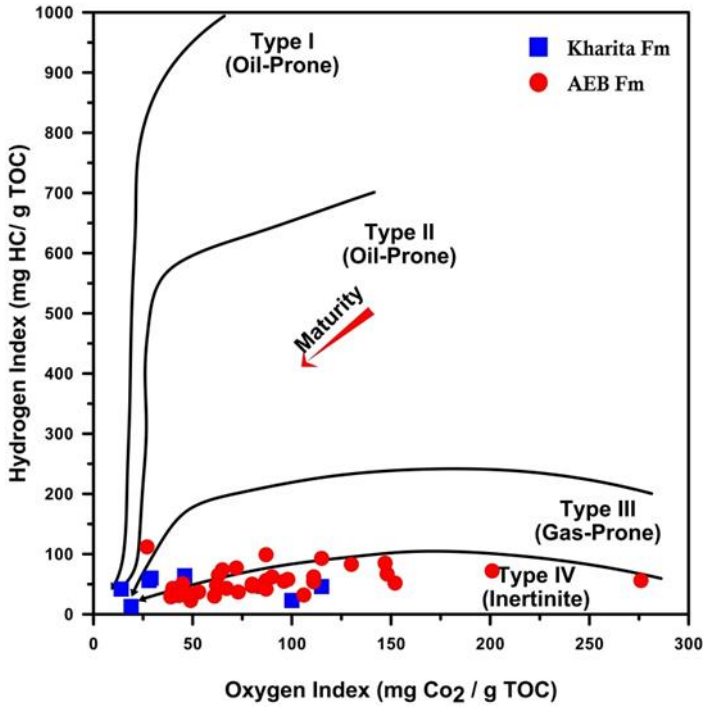

Fig. 4: Cross-plot of studied samples in Tut Oil Field on the HI versus OI kerogen types diagrams.

Table 1: TOC, rock eval pyrolysis, and vitrinite reflectance analysis of the Lower Cretaceous source rocks in the Tut Oil Field, North Western Desert, Egypt.

Well name	*Formation*	*Sample type*	*Depth (ft)*	*TOC (wt %)*	*S1 (mg/g)*	*S2 (mg/g)*	*S3 (mg/g)*	*T_{max} (^{0}C)*	*HI*	*OI*	*PI*	*Calculated R_0*	*Measured R_0*
Tut-21x	Kharita	Cutting	7110	0.68	0.02	0.31	0.78	426	46	115	0.06	0.51	-
			7210	0.85	0.03	0.54	0.39	425	64	46	0.05	0.49	-
			7250	1.40	0.03	0.79	0.39	427	56	28	0.04	0.53	0.52
	Alam El Bueib		8160	0.35	-	-	-	-	-	-	-	-	-
			8170	0.54	0.03	0.28	0.82	426	52	152	0.1	0.51	-
			8180	0.71	0.06	0.59	0.92	429	83	130	0.09	0.56	-
			8190	0.6	0.04	0.4	0.89	438	67	148	0.09	0.72	-
			8230	0.95	0.06	0.94	0.83	429	99	87	0.06	0.56	-
			8240	1.13	0.07	1.05	1.30	430	93	115	0.06	0.58	0.52
			8250	0.93	0.03	0.3	0.98	435	32	106	0.09	0.67	-
			8410	0.70	0.04	0.39	0.61	439	56	87	0.09	0.74	-
			8460	0.77	0.06	0.57	0.50	435	74	65	0.10	0.67	-
			8500	0.88	0.03	0.40	0.73	436	46	83	0.07	0.69	-
			8520	0.85	0.04	0.40	0.68	435	47	80	0.09	0.67	-
			8820	0.92	0.07	0.5	1.02	425	54	111	0.12	0.49	-
			8820	1.52	0.04	0.99	0.96	443	65	63	0.04	0.81	-
			8840	1.05	0.13	0.65	1.17	426	62	111	0.17	0.51	-
			8850	1.08	0.03	0.52	0.67	441	48	62	0.05	0.78	-
			8920	1.32	0.04	1.01	0.95	443	77	72	0.04	0.81	-
			8940	0.85	0.07	0.72	1.25	433	85	147	0.09	0.63	-
			8940	1.13	0.04	0.47	0.98	440	42	87	0.08	0.76	-
			8960	1.04	0.03	0.45	0.69	441	43	67	0.06	0.78	-
			9050	0.63	0.02	0.23	0.46	436	37	73	0.08	0.69	-
			9410	0.79	0.06	0.57	1.59	430	72	201	0.10	0.58	0.67
			9420	0.70	0.04	0.39	1.93	431	56	276	0.09	0.60	-
			10730	3.62	0.12	4.04	0.97	429	112	27	0.03	0.56	0.67
			10770	1.51	0.05	0.93	1.36	431	62	90	0.05	0.60	-
			10780	1.41	0.07	0.77	1.36	425	55	96	0.08	0.49	-
			10830	1.22	0.06	0.61	0.98	428	50	80	0.09	0.54	-
			10860	1.22	0.07	0.71	1.20	431	58	98	0.09	0.60	-
Tut-03	Kharita		7250	0.62	0.16	0.08	0.12	429	13	19	0.67	0.56	-
			7370	0.75	0.42	0.17	0.75	430	23	100	0.71	0.58	-
			7430	0.95	0.12	0.57	0.28	425	60	29	0.17	0.49	-
			7610	1.20	0.05	0.50	0.17	430	42	14	0.09	0.58	-
	Alam El Bueib		8140	1.36	0.03	0.70	0.61	441	51	45	0.04	0.78	-
			8280	1.14	0.02	0.42	0.5	437	37	44	0.05	0.71	-
			8410	1.01	0.02	0.37	0.53	438	37	53	0.05	0.72	-
			8420	1.37	0.08	0.59	0.55	433	43	40	0.12	0.63	-
			8470	1.17	0.03	0.39	0.46	438	33	39	0.07	0.72	-
			8480	1.19	0.03	0.34	0.46	436	29	39	0.08	0.69	-
			8850	1.25	0.04	0.29	0.61	436	23	49	0.12	0.69	-
			8880	1.11	0.04	0.33	0.68	439	30	61	0.11	0.74	-
			8910	1.45	0.04	0.45	0.62	437	31	43	0.08	0.71	-
			8940	1.26	0.04	0.43	0.60	438	34	48	0.09	0.72	-
			8950	1.18	0.04	0.42	0.55	438	35	46	0.09	0.72	-

Note: TOC: total organic carbon; S_1: free hydrocarbons percent in the rock (mg HC/g rock); S_2: residual petroleum potential (mg HC/g rock); HI: hydrogen index (mg HC/g TOC); OI: oxygen Index (mg CO_2/g TOC). T_{max}: the temperature at which the maximum pyrolytic hydrocarbon (S_2) liberated. Ro (%): vitrinite reflectance measurements. PI: production index = $S_1/S_1 + S_2$.

Based on the classification of Peters (1986), Kharita Fm is considered to be fair to good source rocks, and AEB Fm is considered to be a poor- very good source rock (Table 1; Fig. 3) (El Nady and Hakimi, 2016). In addition, the quantity of hydrocarbon yield (S_2) generated during pyrolysis is also a useful indicator to evaluate the hydrocarbon generative potential of the source rock (Peters, 1986; Bordenave, 1993). The pyrolysis yield (S_2) value of the Kharita Fm ranges from 0.08 to 0.79 mg HC/g rock, suggesting poor generating source potential.The studied samples of the AEB Formation have S_2 values ranging from 0.23 to 4.04 mg HC/g rock, reflecting poor to fair source potential (Table 1; Fig. 3).

4.2. Kerogen characteristics and Paleodepositional environments

The present kerogen type was characterised using the results from rock-eval pyrolysis, which included the hydrogen index (HI) and oxygen index (OI) (Table 1). Results of samples collected from Kharita and AEB formations were plotted in HI versus OI on a modified Van Krevelen diagram (Espitalié et al., 1977), this was applied to the organic-rich rocks to classify them (Fig. 4). Considering this plot, the samples from Kharita Fm contain HI and OI values in the range of 13-64 mg HC/g TOC and 14-115 mg CO_2/g TOC, respectively (Table 1). The data was plotted in the field of type III and IV kerogens of terrestrial origin, which have a little gas-prone generative potential (Fig. 4). The hydrogen index (HI) values of the AEB Fm range from 23 to 112 mg HC/g TOC, and the oxygen index (OI) ranges from 27 to 276 mg CO_2/g TOC (Table 1). This indicates mainly a type III kerogen, its generating potential is gas-prone, as shown in Fig. 4.

To find out the kinds of organic matter (OM) in the examined sediments, kerogen microscopy (under transmitted and reflected light) was also used to perform visual kerogen characteristics on a few chosen samples (AEB samples) to give more accurate evaluations of kerogen type, since bulk kerogen type determined by the pyrolysis HI parameter may not always precisely reflect the kinds of hydrocarbons that may be produced by the source rocks and the types of kerogen that are present (Katz, 1983; Hazra et al., 2022).

Palynofacies investigation encompasses the comprehensive examination of all facets of the organic matter assemblage, encompassing the identification of distinct particle constituents, approximation of their absolute and relative quantities, as well as their dimensions and states of preservation (Combaz, 1980). The palynofacies and kerogen macerals data recorded from the AEB Fm are summarized in Table 2. The studied samples were differentiated into three palynofacies assemblages depending on the proportion of the groups of sedimentary organic matter (AOM, phytoclasts, and palynomorphs) (Table 2; Fig. 5; Plate 1).

Palynofacies association-A is dominated by phytoclasts group ranging from 54 to 90%, with significant amounts of amorphous organic matter (6-38%). The palynomorphs are presented in low frequency (Table 2; Fig. 5; Plate 1). Two types of constituents make up the phytoclast portion: minor opaque particles of equant and lath-shaped fragments and dominating, well to moderately preserve structured translucent terrestrial plant fragments. The majority of the amorphous organic matter found there is yellowish-orange to light brown in color. Palynomorphs include dinoflagellates, Foraminifera test linning, spores, and pollens.

Palynofacies association-B reveals a high abundance of phytoclasts (61-98%) compared to palynomorphs and amorphous organic matter. However, Palynofacies association-C displays a dominance of AOM with significant amounts of phytoclasts (Table 2; Fig. 5; Plate 1). The high abundance of AOM in this association is consistent with the detection of mostly liptinite along with vitrinite and inertinite macerals (Table 2; Fig 6). Therefore, based on the microscopic characteristics of the kerogen, it is expected that the shale intervals within the AEB Fm contain different types of kerogen II/III, II and III can generate both oil and gas.

The bulk kerogen characteristics, which indicate kerogen type III, are not supported by this data, as all examined samples have low HI values. The very low hydrocarbon potential may be related to the interaction of the mineral matrix with the produced hydrocarbons, reducing the hydrocarbon yield represented by the S_2 peak, where the hydrocarbons may be adsorbed on the mineral surface and partially released (Katz, 1983; Hazra et al., 2022).

The AEB Fm's palynofacies analysis illustrates various depositional processes connected to eustatic sea level changes and transgression-regression patterns during the deposition period. For this purpose, all samples were plotted on the AOM-phytoclasts-palynomorphs ternary diagram after Tyson (1993) in order to interpret their depositional environments (Fig. 7). The most of the samples of study are located within fields I and II (Tyson, 1995), reflecting a highly proximal shelf to marginal dysoxic-anoxic environment, which represents kerogen Type III that may be gas-prone (Palynofacies association B). On the other hand, some samples are located in field IVa, which indicates a marginal dysoxic-anoxic to shelf to basin transition environment and is characterized as type III and mixed II/III gas-prone kerogen type (Palynofacies association A). Other samples that are assigned to palynofacies association C are located within the VI and VII fields, suggesting a distal dysoxic-anoxic basin, and are classified as type II, oil-prone (Fig. 7).

4.3. Thermal maturation of organic matter

The parameters for foreseeing the thermal maturity of a source rock in the study area are the maximum temperature (T_{max}), the vitrinite reflectance measurements (R_o%), and the production index (PI). The primary phase of hydrocarbon production (the oil generation window) was recorded in 435 °C–465 °C for T_{max}, 0.5%–1.35% for R_o%, and 0.1–0.4 for PI (Espitali'e et al., 1985; Peters, 1986; Peters and Cassa, 1994).

The Kharita Fm has T_{max} and production index (PI) values in the range of 425–430 °C and 0.04–0.71, respectively, indicating that the formation lies in the

immature stage. The cross plots of T_{max}, HI, and PI confirm this result (Table 1; Fig. 8). The high PI values that were observed in some samples of the Kharita Fm suggest an oil contamination effect (Peters, 1986). Alternatively, the AEB Fm has T_{max} and PI values in the range of 425–443 °C and 0.03-0.17, respectively, revealing that the samples lie in immature to mature stages (Table 1; Fig. 8). The removal of some free hydrocarbon content (S_1) during the washing of samples in organic solvent, which was employed to remove the drilling mud additives, may be the cause of the low PI readings in the AEB Formation.

Additionally, the most common method used for determining the stage of maturation is the vitrinite reflectance measurement (R_o %), where it is considered one of the most useful indicators for organic matter maturation (Tissot and Welte, 1984; Bordenave, 1993; El Nady and Hakimi, 2016). The measured R_o% values of Kharita and AEB formations are 0.52 and 0.52-0.67, respectively. These values emphasized the above conclusion (Table 1).

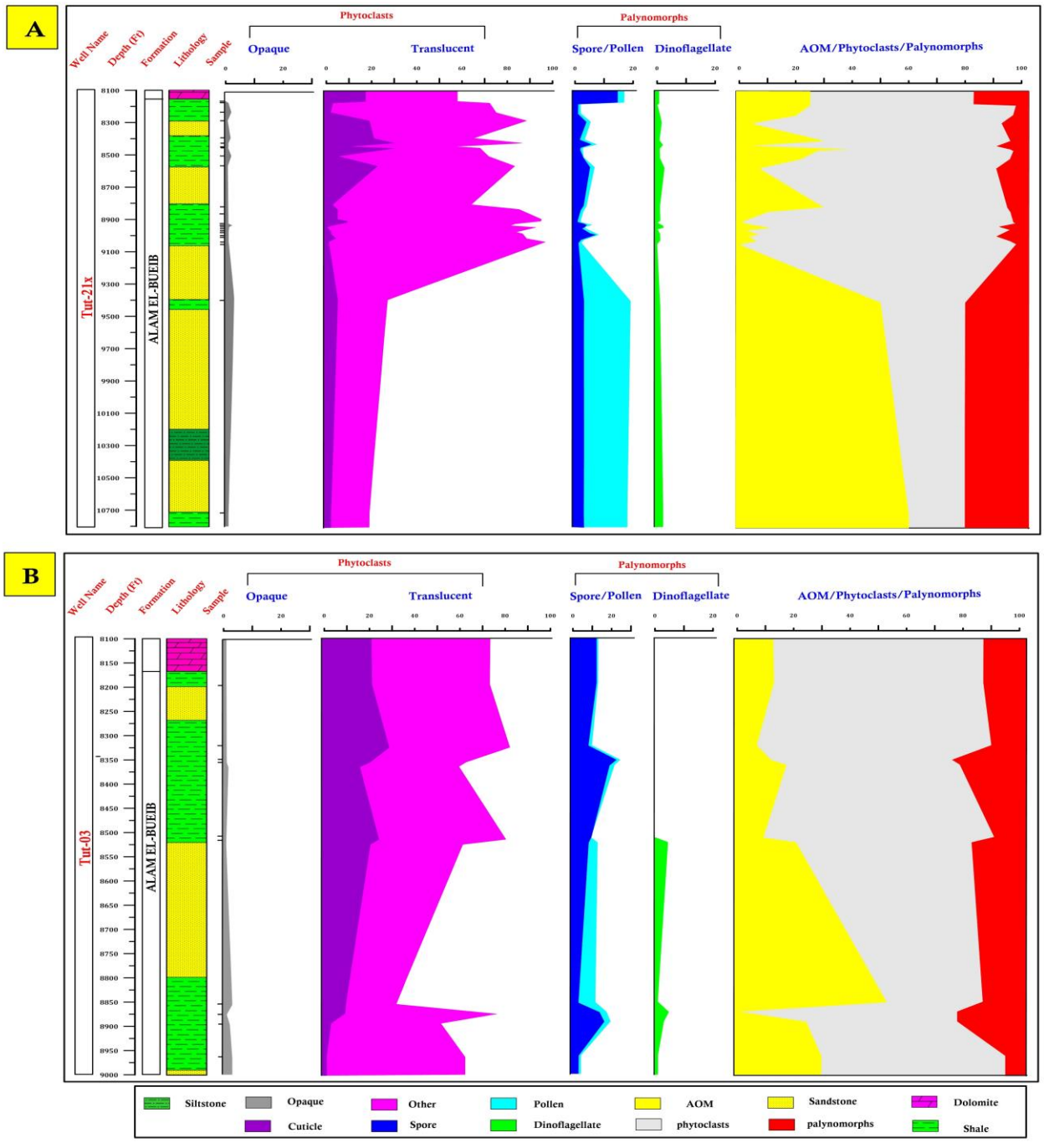

Fig. 5: The relative abundance of the various palynofacies particles plotted against the depth in the AEB Formation in Tut-21x and Tut-3 Wells, North Western Desert, Egypt.

Table 2: Organic petrology results, including palynofacies association and kerogen composition recorded from the Tut-21x and Tut-03 wells.

Well name	Depth (m)	Formation	Palynofacies (%)				Kerogen Composition (%)		
			AOM	Phytoclasts	Palynomorphs	Palynofacies association	Vitrinite	Inertinite	Liptinite
Tut-21x	8180	Alam El Bueib	25	58	17	A			
	8190		25	73	2				
	8250		20	77	3		35	10	55
	8300		4	89	7	B			
	8410		30	66	4	A			
	8440		3	88	9	B			
	8460		38	58	4	A			
	8470		28	69	3				
	8520		22	74	4				
	8580		7	84	9	B			
	8820		30	65	5	A			
	8850		10	86	4				
	8910		1	96	3	B			
	8920		2	96	2				
	8930		5	90	5				
	8940		8	84	8				
	8950		11	83	6	A			
	8960		2	94	4	B			
	8990		7	85	8				
	9000		3	88	9				
	9030		6	90	4	A			
	9050		0	98	2	B			
	9410		50	30	20	C	20	10	70
	10730		60	20	20		30	5	65
Tut-03	8190		13	74	13	B			
	8320		7	83	10				
	8350		12	64	24				
	8360		18	61	21				
	8510		10	81	9	A			
	8520		21	62	17				
	8850		52	35	13	C			
	8870		0	78	22	B			
	8890		24	54	22	A			
	8960		30	65	5				

Plate 1: Bright field-transmitted light photomicrographs of selected amorphous organic matter (AOM), phytoclasts, and palynomorphs from the AEB Formation, Tut Oil Field. The well name and corresponding depth follow the identification of each specimen. Size information is given by a scale bar on the image. (1–3) AOM particles. Note the association of the black pyrite crystals, indicating reducing conditions. Image 1 is from Tut-21x, 8180 ft; image 2 is from Tut-21x, 8520 ft; and image 3 is from Tut-21x, 8460ft. (4) Equant opaque particle. Such equidimensional opaques usually indicate a longer distance of transportation. Tut-21x, 8180 ft. (5) Lath-shaped opaque particle. Tut-21x, 8250 ft. (6,7) Translucent cuticle phytoclasts. Image 6 is from Tut-21x, 8850 ft; image 7 is from Tut-21x, 8300 ft. (8) Translucent tracheid phytoclast. The presence of well-defined bordered pits clearly indicates a gymnosperm origin. Tut-21x, 8580 ft. (9) Lath-shaped tracheid, Equidimintional in form, derived probably from gymnosperms. Tut-21x, 8580 ft. (10) spore. Tut-21x, 8180 ft. (11) spore. Tut-21x, 8470 ft. (12) pollen. Tut-03, 8870 ft. (13) pollen. Tut-03, 8850 ft. (14) Planispiral microforaminiferal inner test lining. Tut-21x, 8850 ft. (15) Dinoflagellate cyst. Tut-03, 8850 ft. (16) Uniserial tectinous foraminiferal test linings. Tut-21x, 8440 ft.

4.4. Maturation and petroleum generation model

The amount and timing of petroleum production from the prescribed source rocks are summarized in Fig. 9. In this study, the measured R_o% of the Jurassic-Cretaceous source rock in the deeper well in the study area (Tut-21x) was applied in order to adjust the thermal maturity models. The study's thermal maturity model is valid, as indicated by the very strong correlation between the measured and modelled R_o% values.

As shown in Fig. 9, the source rocks of AEB entered the early mature stage of oil generation during the Upper Cretaceous age at 89.22–79.39 Ma (before present), and oil generation has not yet reached its peak . Conversely, the Khatatba and Yakout source rocks entered the oil generation zone at 70 Ma and 122.78 Ma, respectively. Yakout source rock reached the peak of oil generation at 82.67 Ma, still in the present day at this stage.

There was just one stage that reflected the hydrocarbon generation and history of expulsion of the AEB source rocks in the examined well (Tut-21x). No generation or expulsion is noticed, where the transformation ratio (TR) of the source rocks is <10%. Their lower thermal maturity level and lesser burial depth are the causes of this. This stage took place between 92 Ma from the Late Cretaceous to the Current Period (Fig. 9C) (El Nady and Hakimi, 2016).

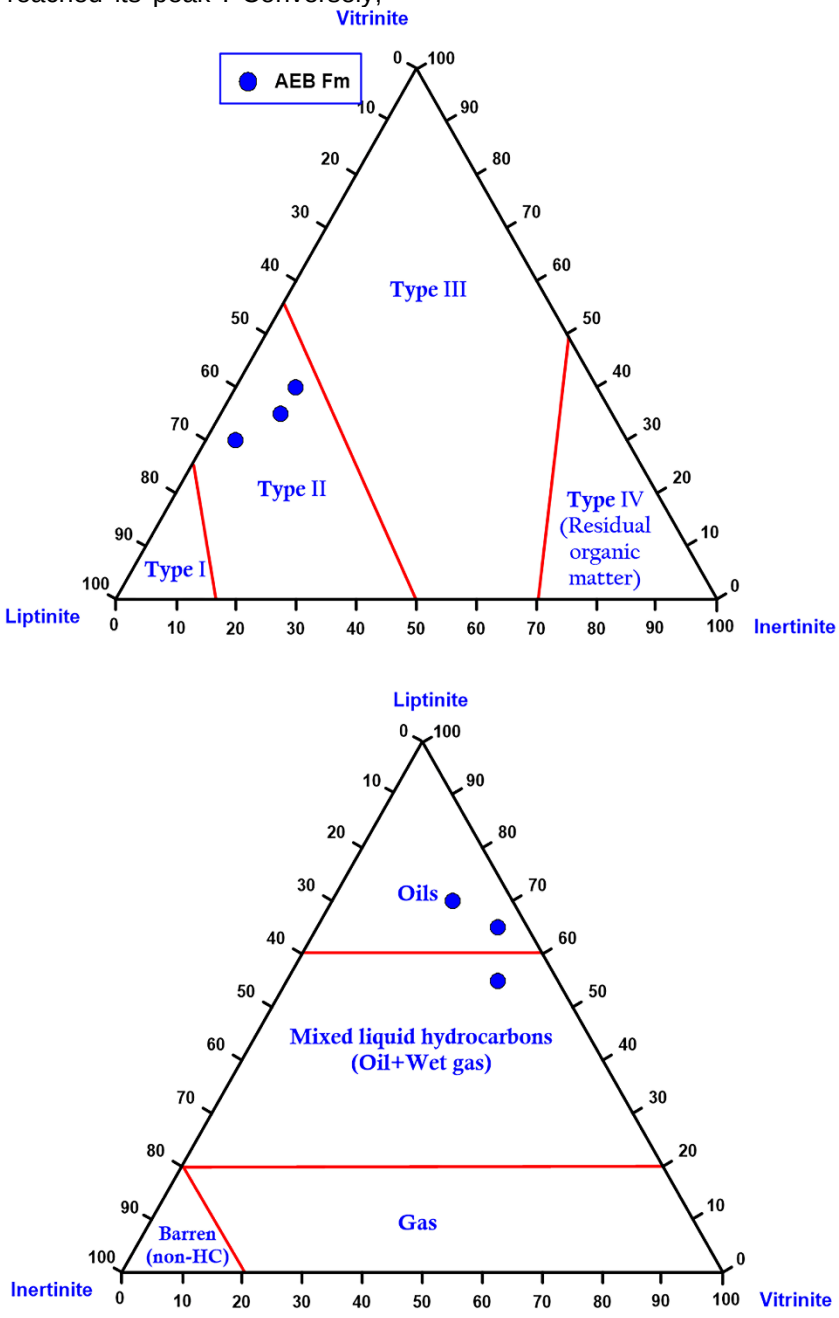

Fig. 6: Vitrinite, liptinite, and inertinite ternary plots of the studied samples to identify organic matter quality

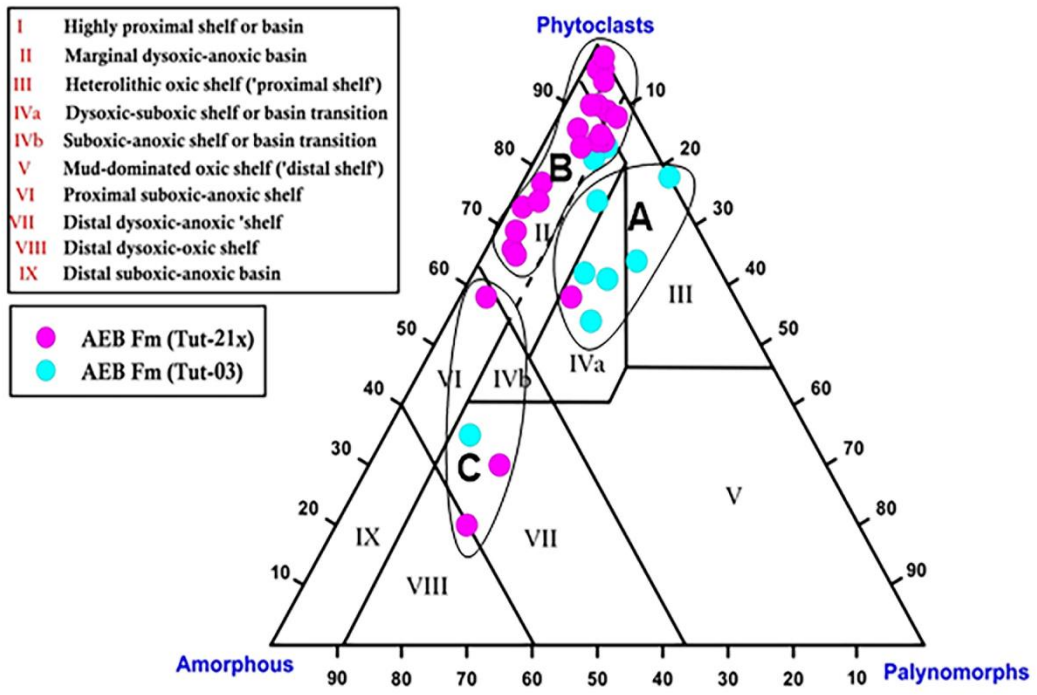

Fig. 7: AOM-Phytoclast-Palynomorph ternary plot of the studied samples of the Tut Oil Field.

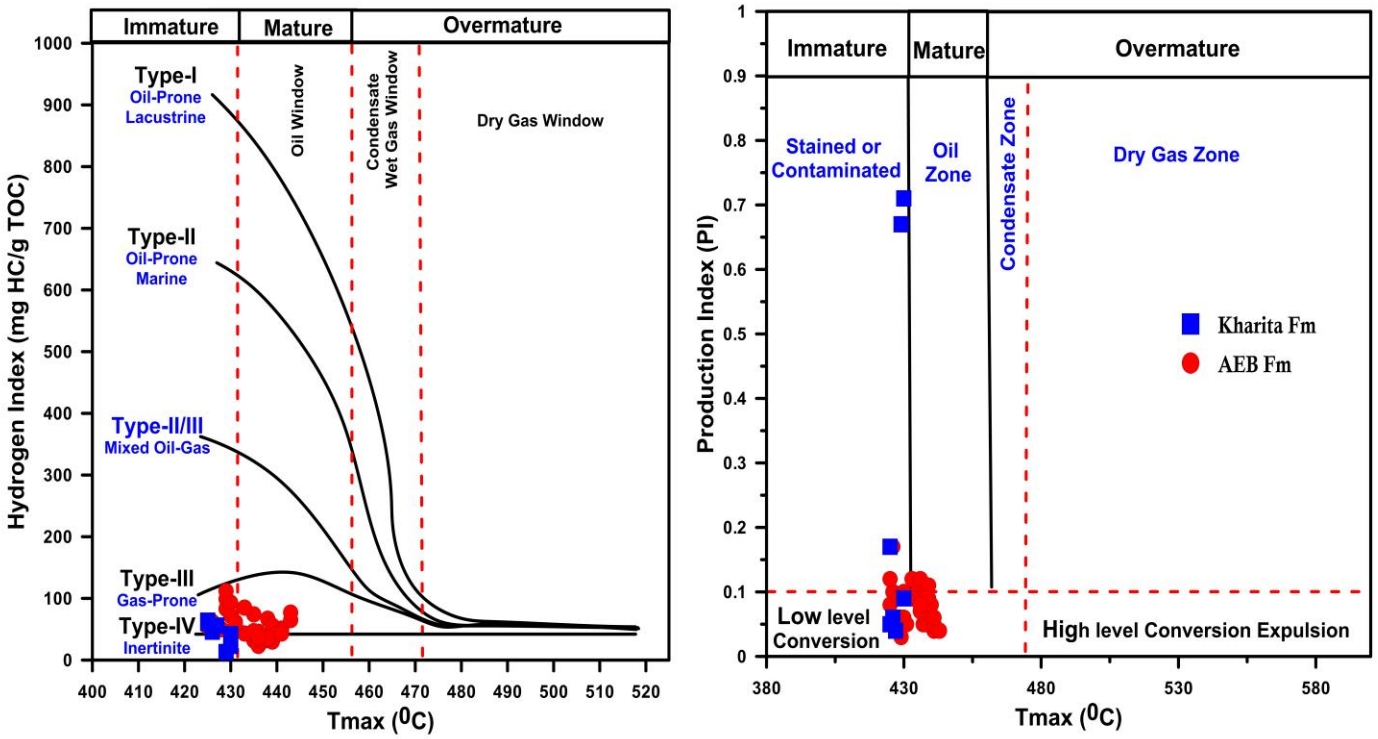

Fig. 8: A) T_{max} versus HI and **B)** T_{max} versus PI cross plots of the studied formations in Tut Well, North Western Desert, Egypt.

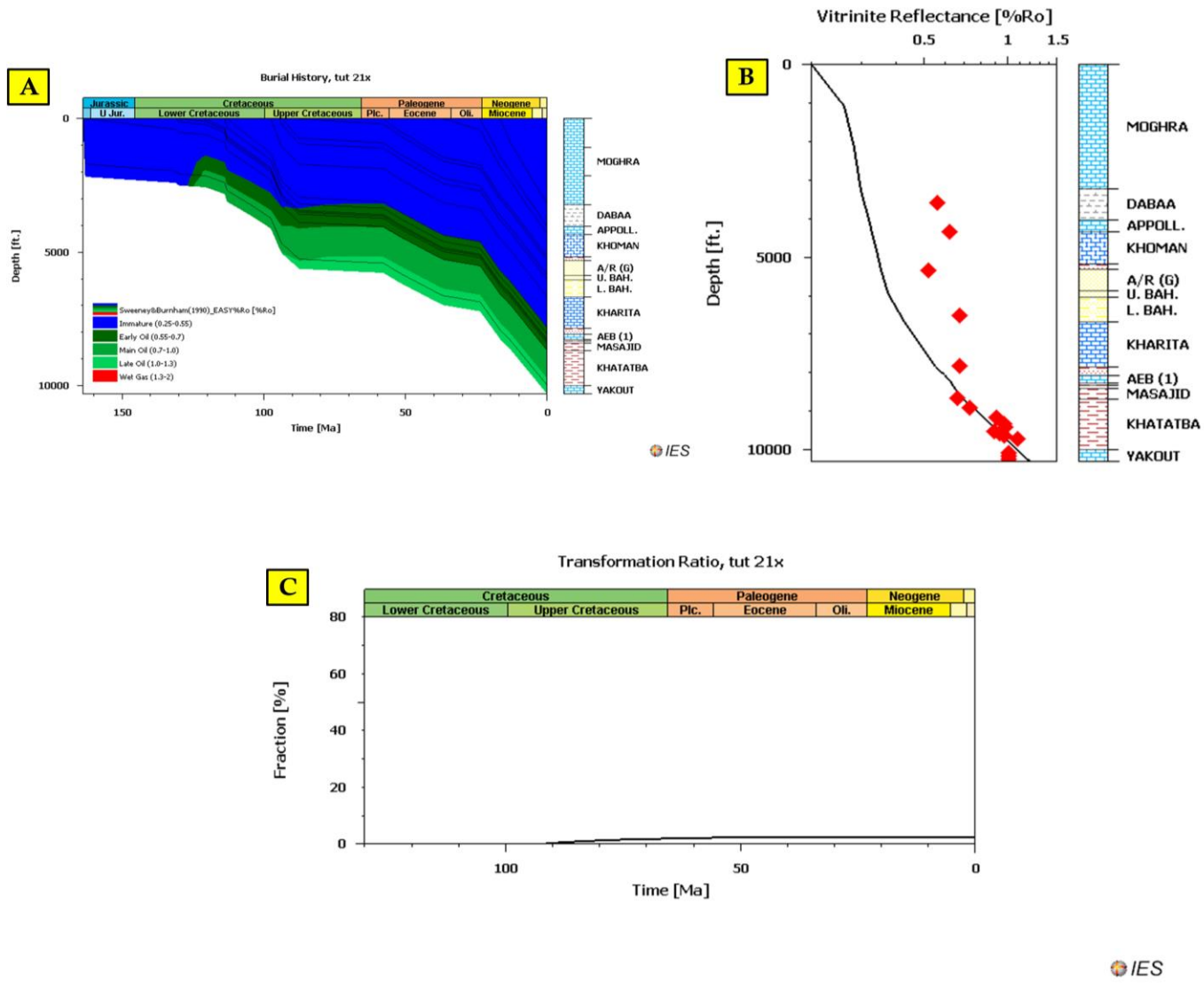

Fig. 9: A) Thermal maturity histories for the studied Tut-21x well; **B)** The depth vs. measured vitrinite reflectance data that correlated to the modeled curve (solid black line); **C)** Evolution of the transformation ratio of AEB Fm in the studied well.

Conclusions

Thorough organic geochemical and petrographic analyses of Lower Cretaceous source rocks in Tut Oil Field have been used to evaluate organic matter properties, ascertain the Kharita and AEB formations' depositional environment, and track the timing and expulsion of hydrocarbons from these source rocks. The study's findings indicate the following:

1. Kharita Formation is an immature with poor generating potential source rock for generating gas (type III and IV kerogens).
2. The AEB Formation bears immature to mature source rocks and has poor to very good generating capability for generating oil (type II), oil/gas (type II/III), and gas (type III kerogen).
3. A wide variety of palynofacies associations indicating various depositional settings and kerogen types are found in the AEB Formation, including a highly proximal shelf to marginal dysoxic-anoxic environment, a marginal dysoxic–anoxic to shelf to basin transition environment, and a distal dysoxic-anoxic basin.
4. The source rocks of AEB entered the early mature stage of oil generation during the Upper Cretaceous age at 89.22–79.39 Ma (before present), and they have not yet achieved their peak oil-producing stage.

References

Barakat, M.G., (1982). General review of petroliferous provinces of Egypt with special emphasis on their geological setting and oil potentialities. Energy Project, Petroleum and Natural Gas Project, Cairo Univ., M.I.T. Technical Planning Program, Cairo. Egypt, 34-56.

Bordenave, M.L., (1993). Applied Petroleum Geochemistry. Editions Technip, Paris.

Combaz, A., (1980). Les Kérogènes vus au microscope. In: Durand, B. (Ed.),

Kerogen: insoluble organic matter from sedimentary rocks. Edition Technip, Paris, 55-111.

EGPC, (1992). Western Desert, oil and gas fields, a comprehensive overview. 11th Egyptian General Petroleum Corporation Exploration and Production Conference, Cairo, 1-431.

El Nady, M.M. and Hakimi, M.H., (2016). The petroleum generation modeling of prospective affinities of Jurassic–Cretaceous source rocks in Tut oilfield, north Western Desert, Egypt: an integrated bulk pyrolysis and 1D-basin modeling. Arabian Journal of Geosciences, 9 (6), 1-14.

El Nady, M.M., (2001). Nature and origin of hydrocarbon for some middle Jurassic-Lower Cretaceous of the Meleiha area in the North Western Desert, Egypt. J. Egypt. Pet. 10, 91–109.

Espitalie, J., Deroo, G. and Marquis, F., (1985). Rock-Eval pyrolysis and its applications. Revue De L Institut Francais Du Petrole, 40(5), 563-579.

Espitalié, J., La Porte, J.L., Madec, M., Marquis, F., Le Plat, P., Paulet, J. and Bautefeu, A., (1977). Methodé rapide de caractérisation des roches mères de leur potential potential pétrolier et de leur degre d' évolution. Revue de l'Institut Français du pétrole, 32, 23-42.

Hazra, B., Katz, B.J., Singh, D.P. and Singh, P.K., (2022). Impact of siderite on Rock-Eval S3 and oxygen index. Marine and Petroleum Geology, 143, 105804.

Huang, W.H., Ao, W.H. and Weng, C.M., (2010). Characteristics of coal petrology and genesis of Jurassic coal in Ordos Basin. Geoscience, 24, 1186–1120.

Hunt, J.M. (1995). Petroleum geochemistry and geology (textbook). Petroleum Geochemistry and Geology (Textbook). (2nd Ed.), WH Freeman Company.

Katz, B.J., (1983). Limitations of 'Rock-Eval'pyrolysis for typing organic matter. Organic Geochemistry, 4(3-4), 195-199.

May, R.M., (1991). The Eastern Mediterranean Mesozoic Basin: evolution and oil habitat. AAPG Bull., 75, 1215–1223.

Pepper, S.A. and Corvi, J.P., (1995). Simple kinetic models of petroleum formation. Part I: oil and gas generation from kerogen. Marine and Petroleum Geology, 12(3), 291-319.

Peters, K.E. and Cassa, M.R., (1994). "Chapter 5: Applied Source Rock Geochemistry", in the petroleum system- from source to trap, edited by Magoon, L. B., and Dow, W. G., AAPG memoir 60, 93-120.

Peters, K.E., (1986). Guidelines for evaluating petroleum source rock using programmed pyrolysis. AAPG Bulletin, 70(3), 318–329.

Ramadan, F.S., Metwalli, F.I., El-Khadragy, A.A. and Afify, W., (2012). The subsurface geology and source rocks characteristics of some Alam El Bueib reservoirs in Tut oil field, north Western Desert, Egypt. Journal of Applied Sciences Research, 8(11), 5388-5409.

Said, R., (1990). The Geology of Egypt, A.A., Balkema, Rotterdam, Brookfield, 734 pp.

Shalaby, M.R., Hakimi, M.H. and Abdullah, W.H., (2012). Organic geochemical characteristics and interpreted depositional environment of the Khatatba Formation, northern Western Desert, Egypt. AAPG Bulletin, 96, 2019-2036.

Shalaby, M.R., Hakimi, M.H. and Abdullah, W.H., (2013). Modeling of gas generation from the Alam El-Bueib formation in the Shoushan Basin, northern Western Desert of Egypt. Int J Earth Sci (Geol Rundsch), 102, 319-332.

M. R. Sharaf, L. M., and El Nady, M. M. 2003. Geochemical characterization of source rocks and oil-source rocks correlation in some wells within South Umbarka area, north Western Desert, Egypt. J. Sedimentol. Egypt 11, 61–76.

Sultan, N. and Abdelhalim, M., (1988). Tectonic framework of northern Western Desert, Egypt and its effect on hydrocarbon accumulation, 9th EGPC Expl. Conf.CONOCO

Temraz, M.G., Mandur, M.M. and Coffey, B., (2016). Reservoir sedimentology and depositional environment studies of Alam El Bueib Formation using microfacies and nannofossils in Betty-1 well, Shoushan Basin, northern Western Desert, Egypt. Environmental Geosciences, 23(3), 123-139.

Tissot, B.P. and Welte, D.H., (1984). Petroleum formation and occurrence. 2nd Ed. Springer-Verlag, Berlin, 200 p.

Traverse, A., (2007). Paleopalynology: Topics in Geobiology 28 (second edition): Rotterdam, Springer, 813 p., doi: 10.1007 /978-1-4020-5610-9.

Tyson, R.V., (1993). Palynofacies analysis, in Jenkins, D.G., ed., Applied micropaleontology: Dordrecht, Netherlands, Kluwer Academic Publishers, 153–191 p.

Tyson, R.V., (1995). Sedimentary organic matter: Organic facies and palynofacies: London, Chapman and Hall, 615 p.

Yasser, A., Leila, M., El Bastawesy, M. and El Mahmoudi, A., (2020). Petrophysical evaluation of lower Cenomanian Bahariya reservoir, Salam oil field, Shushan basin, north Western Desert, Egypt. Journal of Environmental Sciences. Mansoura University, 49(4), 99-105.